Damping Response Analysis of T-shaped Structure Containing New Acoustic Black Hole with Residual Thickness Supported by a Nonlinear Concentrated Spring

Koki Yamaguchi[1,a], Takao Yamaguchi[1,b*], Koki Mitsumata[1],
Chihiro Kamio[1,c] and Shinichi Maruyama[1,d]

[1]Division of Electronics and Mechanical Engineering, Gunma University,
1-5-1 Tenjin-cho, Kiryu, Gunma 376-8515, Japan

*Corresponding author

[a]<t252b610@gunma-u.ac.jp>, [b]<yamagme3@gunma-u.ac.jp>, [c]<chihiro.kamio@gunma-u.ac.jp>,
[d]<maruyama@gunma-u.ac.jp>

Keywords: acoustic black hole, residual thickness, nonlinear spring, damping, finite element method, vibration suppression, earthquake engineering

Abstract. We proposed a lightweight, highly vibration damping structure using a new acoustic black hole that solves problems of weakness in strength. Rather than plate thickness, the acoustic black hole function was used for the height of ribs in T-shaped structures. Nonlinear vibration analysis using finite element method with Model Strain Energy Method were carried out for T-shaped steel structures supported by a nonlinear concentrated spring under impact load. The T-shaped steel is composed of steel layer having an “acoustic black hole” with residual thickness. A viscoelastic damping layer is covered on the acoustic black hole. We calculated modal loss factors and nonlinear transient responses. We clarified effects of an “acoustic black hole” with residual thickness and nonlinear springs on the nonlinear damped responses.

1. Introduction

In recent years, earthquakes have occurred frequently, and structures have collapsed. The most common solution is to increase natural frequencies by reducing weight of the structure or increasing their rigidity, but lightweight structures often cause dangerous resonance phenomena due to its lack of rigidity. To evaluate the nonlinearity of the soil during strong earthquakes, nonlinear impact response analysis plays critical role in avoiding coupling between structural vibration modes and soil behavior.

One approach for effective damping method in a confined space is to use “acoustic black hole” proposed by Mironov [1]. This damping method utilizes the non-reflective condition of vibration propagating toward the wedge-shaped steel plate whose tip end thickness decreases with power series greater than the quadratic function, which is equivalent to the wave propagation over a long distance. In other words, as the plate thickness decreases toward the end of the plate, the wavelength of the bending wave becomes shorter. When the plate thickness decreases as a power function of a quadratic or higher function, the wavelength becomes infinitely short and cannot reach the end of the plate. Due to this phenomenon, the end of the plate with an acoustic black hole becomes a non-reflecting end. Krylov [2-5] showed that a thin viscoelastic damping layer on the wedge-shaped steel plate increases damping coefficient of the plate effectively based on the theory of Oberst [6], which contributes to shortening the tip length of the acoustic black hole. Tang et al. [12] proposed a structure that incorporates a tunnel-shaped acoustic black hole inside the plate. Deng et al. [13] calculated sound transmission loss of a plate incorporating multiple acoustic black holes in two dimensions, like craters. Deng et al. [14] also proposed a method of attaching the plate with multiple crater-shaped acoustic black holes as an additional structure to the target structure.

However, the edges of conventional acoustic black hole are very thin and sharp, and then it is difficult to adopt actual structures because of their strength. We proposed a lightweight, highly vibration damping structure using a new acoustic black hole that solves these problems. Rather than plate thickness, the acoustic black hole function was used for the height of ribs in T-shaped structures.

Previously, Yamaguchi et. al. [8-10] proposed a fast calculation method and clarify the nonlinear vibrations in elastic / viscoelastic blocks or a sound-proof structure with nonlinear concentrated springs with linear hysteresis. In these investigations, we used modal loss factors computed from Modal Strain and Kinetic Energy method (i.e. MSKE method) [11]. This MSKE method is extended version from Modal Strain Energy method (i.e. MSE method) [15-16]. Using the modal loss factors and modal parameters, nonlinear impact responses can be computed from nonlinear ordinary simultaneous equations as to normal coordinates corresponding to linear eigenmodes. Using this, we studied effects of the acoustic black hole on the vibration of structures supported by nonlinear springs [11]. However, in this investigation, because there exists not only an acoustic black hole but also viscoelastic damping layers on the flanges in the structures, both effects were mixed on the responses. To separate these effects, we removed viscoelastic damping layers on the flanges in this report. Then, we clarified purely damping effects of the acoustic black hole on the nonlinear impact responses.

Under the above conditions, we investigate effects of acoustic black hole with/without residual thickness proposed by Liling TANG [7] for T-shaped steel on modal loss factors. We also discussed nonlinear impact responses of the model supported by a nonlinear concentrated spring in the vertical direction.

2. Analytical Model

Fig.1 shows the analytical model of the T-shaped steel structure. As a numerical example, we set three conditions for (a) Base model (with acoustic black hole), (b) Residue model (with acoustic black hole having residual thickness), and (c) Comparative model (without acoustic black hole) to investigate the effect of acoustic black hole with residual thickness supported by a nonlinear concentrated springs on modal loss factor and nonlinear impact analysis.

Base model is the baseline condition of T-shaped steel structure with acoustic black hole, as shown in Fig. 1(a). To introduce the acoustic black hole into the T-shaped structure, we set the height $H(x) = \varepsilon x^{2.2}$of the rib which decrease by a 2.2-th order power function toward the tip end as shown in Fig. 2. This 2.2-th order function is the same with reference to the modeling by Krylov [2-5]. The thickness of the laminated viscoelastic damping layer is set to 10 [mm]. For Residue model, residual thickness [7] was added to Base model as shown in Figs. 1(b) and 2. Residual thickness means that thin plate stretched with a constant minimum thickness at the tip end of an acoustic blackhole. This residual thickness plays a role of damping for longer wave length. Comparative model is the standard T-shaped structure composed of a plate as flanges and a beam without acoustic black hole and without residual thickness (Fig. 1(c)).

Regarding the coordinate system of the model, we set x-axis in longitudinal direction, y-axis in height direction, and z-axis in width direction. The linear concentrated springs were installed at the boundary between the acoustic black hole portion and the T-shaped structure portion of each model in the x and z axis. One nonlinear concentrated spring was set only in the y-axis direction as shown in Fig. 1. The nonlinear concentrated spring had the third order hardening restoring force, whose linear components are complex modulus expressed as follows.

$$\gamma_{1my} = \overline{\gamma}_{1my}(1 + j\eta_s) \tag{1}$$

Where, j is the imaginary unit. We set $\overline{\gamma}_{1my}$=12.0 [N/mm], η_s=0.01 [-], $\overline{\gamma}_{2my}$=0.00 [N/mm^2] which represents the nonlinear spring constant for the quadratic term. and $\overline{\gamma}_{3my}$=12.0 [N/mm^3] which is the nonlinear

spring constant for the cubic term. This nonlinear spring with hysteretic damping represents a spring that stiffens when compressed. It is suitable for polymeric materials and soils that stiffen under compression. The T shaped-structures are clamped at the opposite end to the acoustic blackhole as shown in Fig. 3.

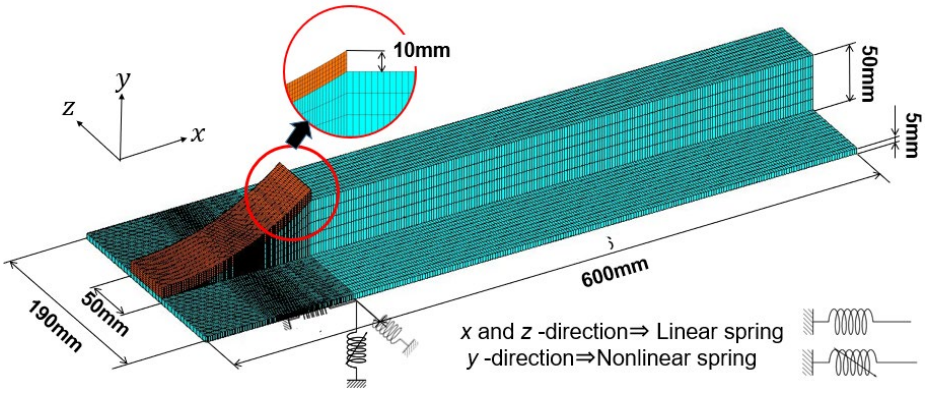

(a) Base model (with acoustic black hole)

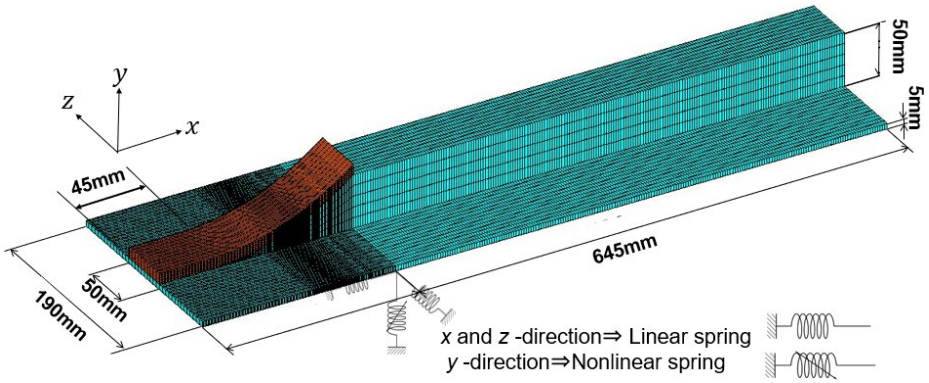

(b) Residue model (with acoustic black hole having residual thickness)

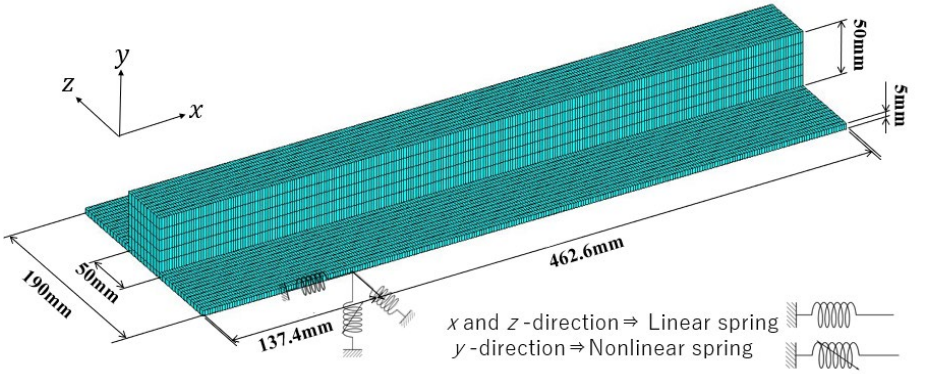

(c) Comparative model (without acoustic black hole)

Fig. 1. Analytical model of T-shaped steel structure.

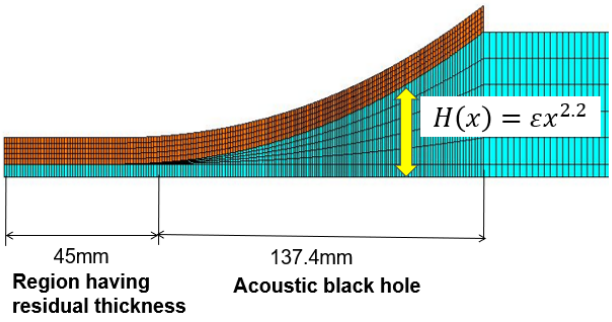

Fig. 2. Acoustic black hole with residual thickness with viscoelastic damping layer in Residue model.

As illustrated in Fig. 4, the excitation point was set to the boundary between the acoustic black hole portion and the T-shaped structure portion. And the observation point was set above the excitation point.

Material properties are listed in Table1.

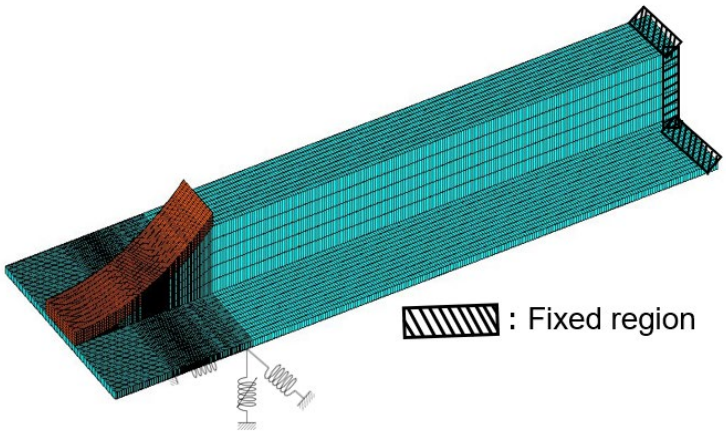

Fig. 3. Boundary condition.

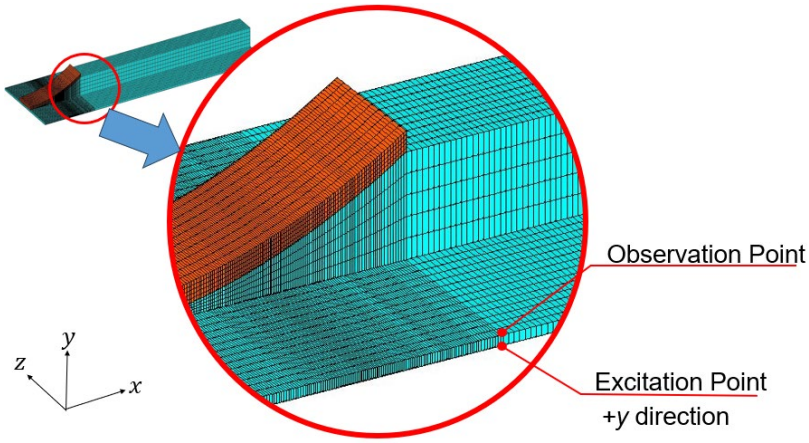

Fig. 4. Excitation point and observation point.

Table 1. Material properties.

	Young's modulus [Pa]	Mass density [kg/m^3]	Poisson's ratio [−]	Material loss factor [−]
Steel	2.1×10^{11}	7.8×10^3	0.33	0.001
Viscoelastic damping material	8.0×10^8	1.4×10^3	0.45	0.333

3. Numerical Calculation Method

The edge of the spring elements is connected to the node of the model a_m $(m = 1)$, considering the elastic p rincipal axis coincides with the spring direction in this study.

3.1 Discretization equation for nonlinear concentrated spring

The nodal force of the m-th nonlinear concentrated spring is a hardening nonlinear spring and is expressed as a series of the third order of displacement U_{my} $(m = 1)$ as follows.

$$R_{my} = \gamma_1 U_{my} + \gamma_3 U_{my}^3 \tag{2}$$

These relations can be rewritten in the matrix form as follows:

$$\{r_m\} = [\bar{\gamma}_{1m}]\{U_s\} + \{\bar{d}_m\} \tag{3}$$

where $\{r_m\}$, $[\overline{\gamma}_{1m}]$, and $\{\overline{d}_m\}$ denote the nonlinear spring restoring force vector, complex stiffness matrix involving only the linear term of the restoring force γ_{1m}, and the vector containing the nonlinear terms of the restoring force. γ_1 is the complex modulus for linear hysteresis damping.

3.2 Discretization equations for models

By superposing the strain energy, kinetic energy, and potential energy of elements related to the structure, the following equations in the entire domain of the system are obtained from the Lagrange equation:

$$[M_s]\{\ddot{U}_s\} + [K_s]\{U_s\} = \{f_s\} \tag{4}$$

where $[M_s]$, $[K_s]$, $\{U_s\}$, and $\{f_s\}$ denote the mass matrix, complex stiffness matrix, nodal displacement vector, and nodal force vector of the structure, respectively. Note that the complex modulus of elasticity is defined as the hysteresis damping for the viscoelastic damping layer.

3.3 Discretization equation for T-shaped structures with a nonlinear spring

The following equations can be obtained for the global system, by adding the nonlinear spring restoring force vector $\{r_m\}$ in Eq. (1) to nodal force at the attached nodes a_m $(m = 1)$ in Eq. (4):

$$[M]\{\ddot{U}\} + [K]\{U\} + \{\hat{d}\} = \{f\} \tag{5}$$

where $[M]$, $[K]$, $\{U\}$, and $\{f\}$ denote the mass matrix, complex stiffness matrix, nodal displacement vector, and nodal force vector for the global system, respectively. $\{\hat{d}\}$ is the vector obtained by modifying $\{\bar{d}\}$ to have a vector size for global system.

3.4 Conversion to nonlinear discretization equations in normal coordinates

To diminish the degree of freedom for the discrete equation of motion, normal coordinates are introduced corresponding to the linear complex natural modes. Note that we assume that the linear complex natural modes of vibration $\{\phi^{(i)}\}$ can be approximated to real eigen modes $\{\phi^{(i)}\}_0$. The nonlinear ordinary simultaneous equations regarding the normal coordinates are as follows:

$$\ddot{\tilde{b}}_i + \eta_{tot}^{(i)}\omega^{(i)}\dot{\tilde{b}}_i + \left(\omega^{(i)}\right)^2\tilde{b}_i + \sum_j\sum_k \tilde{E}_{ijkl}\,\tilde{b}_j\tilde{b}_k\tilde{b}_l = \tilde{P}_i$$

$$\tilde{E}_{ijkl} = \sum_m \gamma_{3my}\frac{n_i}{n_j n_k n_l}\tilde{\phi}_{imy}\tilde{\phi}_{jmy}\tilde{\phi}_{kmy}\tilde{\phi}_{lmy},$$

$$\tilde{P}_i = n_i\{\tilde{\phi}^{(i)}\}_0^T\{f\} \tag{6}$$

where $\eta_{tot}^{(i)}$ denote the *i*-th modal loss factor, calculated by Modal Strain Energy (MSE) method with the share of the strain energy of each element to the total strain energy.

Nonlinear impulse responses were computed using Runge-Kutta-Gill method in Eq. (6). In this numerical integration, an impulse was set for the force vector $\{f\}$ in Eq. (6) at the node β, which is the excitation point. By changing the maximum amplitude $|f_{max}|$ of the impact under a constant pulse width 0.001 [s], we calculate nonlinear transient time histories.

4. Numerical Calculation results

4.1 Eigen value analysis results

Fig. 5 shows the modal loss factors calculated by Base model (with acoustic black hole), Residue model (with acoustic black hole having residual thickness), and Comparative model (without acoustic black hole). To investigate the damping effect on the lower frequency range, average values of modal loss factor less than 1000 [Hz] are listed in Fig. 5.

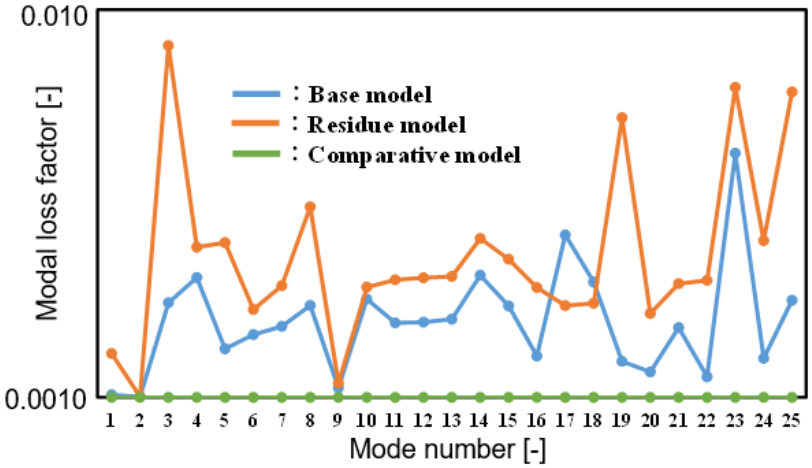

Fig. 5. Modal loss factor calculated by Base model (with acoustic black hole), Residue model (with acoustic black hole having residual thickness), and Comparative model (without acoustic black hole).

As we can see in Fig. 5, the modal loss factor increased in Base model (with acoustic black hole) compared to that in Comparative model (without acoustic black hole). In Residue model (with acoustic

black hole having residual thickness), the modal loss factor becomes higher than that in Base model (with acoustic black hole). These results showed that acoustic black hole with residual thickness increases the modal loss factor.

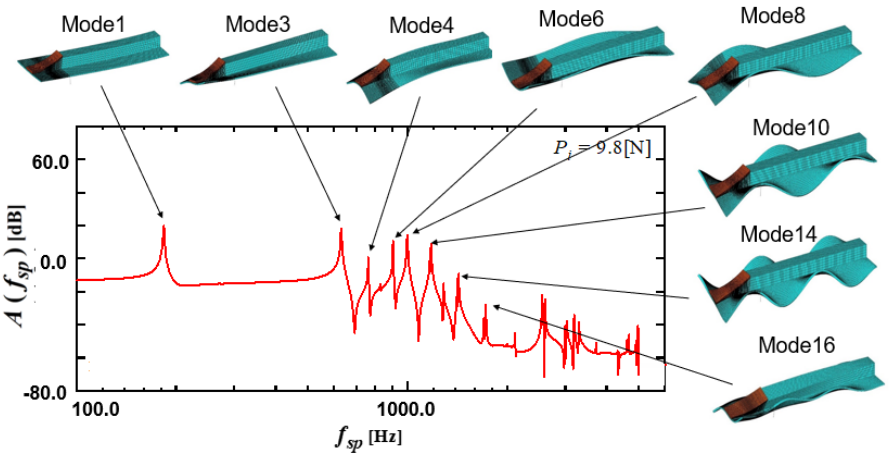

(a) Base model (with acoustic black hole)

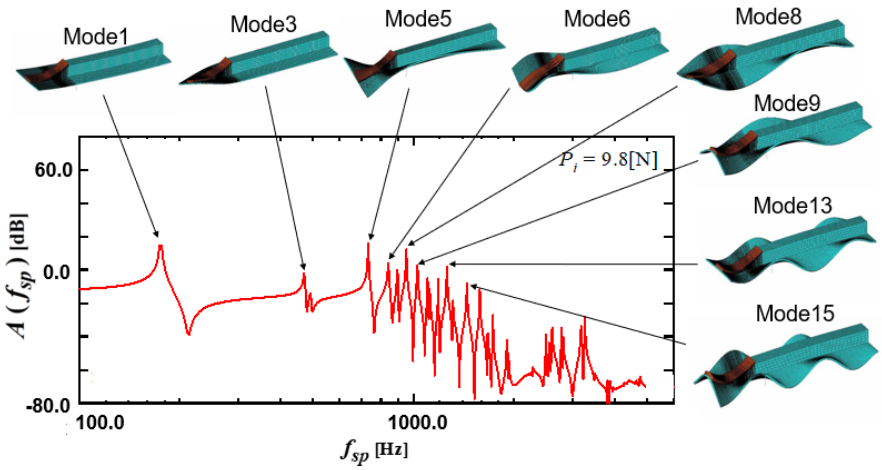

(b) Residue model (with acoustic black hole having residual thickness)

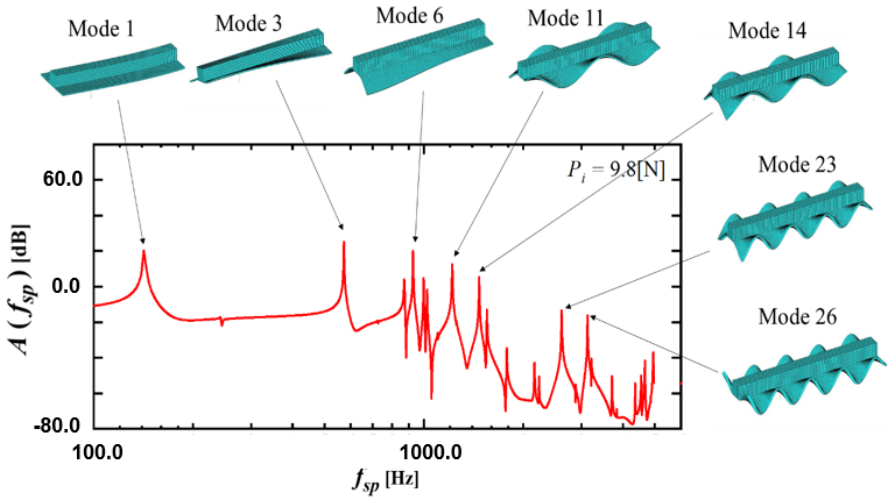

(c) Comparative model (without acoustic black hole)

Fig. 6. Fourier spectrum of impact responses under small input (9.8 [N]).

Fig. 6 shows impact responses under small excitation force 9.8 N. Dominant peaks due to resonances appear in the response curves. Under this small excitation force, these responses can be regarded as linear responses. Especially, the peak level of Residue model (with acoustic black hole having residual thickness) for Mode 3 is smaller than that of Base model (with acoustic black hole) due to the damping effect of introducing residual thickness. This residual thickness gives higher damping for Mode3 having the long wave length.

The peak level of Residue model (with acoustic black hole having residual thickness) for Mode 3 is much smaller than that of Comparative model (without acoustic black hole).

Next, we increased the excitation force and examined modal coupling in the impact responses.

As an example, we show the results of the base model with the acoustic black hole in Fig.6.

Comparing the cases where the excitation force is 9.8 N with the case where the excitation force is 980 N, we can see that by increasing the excitation force, spectra that were not present in the basic response at 9.8 N appear. There exist new many peaks and sideband due to the nonlinear effects under large input 980N. These are thought to be the effects of the harmonic and subharmonic components of the resonance, which correspond to modes where deformation of the nonlinear spring is large. It is clearly found that there is the third order super harmonic component at 2007Hz of Mode 3 (637Hz), which includes the large deformation in the nonlinear spring. The third order super harmonic component of Mode 3 is generated from the component of the restoring force $[\gamma_3(e^{j\omega^{(3)}t})^3 = \gamma_3 e^{j3\omega^{(3)}t}]$ of the nonlinear spring in Eq. (2).

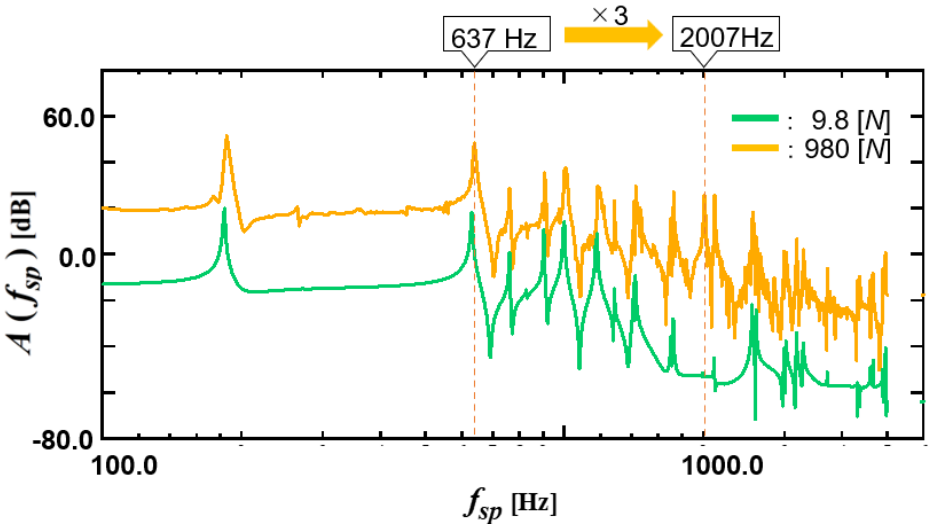

Fig. 7. Change in Fourier spectrum of impact responses from small input to large input for Base model (with acoustic black hole).

Next, we compared impact responses for three cases under large input 980N. As shown in Fig. 8, there exist complicated fractional harmonic components in each impact response under the larger input than those under the small input in Fig. 6. In comparison of Comparative model (without acoustic black hole), the amplitude of the proposed structure with acoustic black holes (Base model and Residue model) are diminished for the overall nonlinear vibration peak, specifically in the higher frequency range.

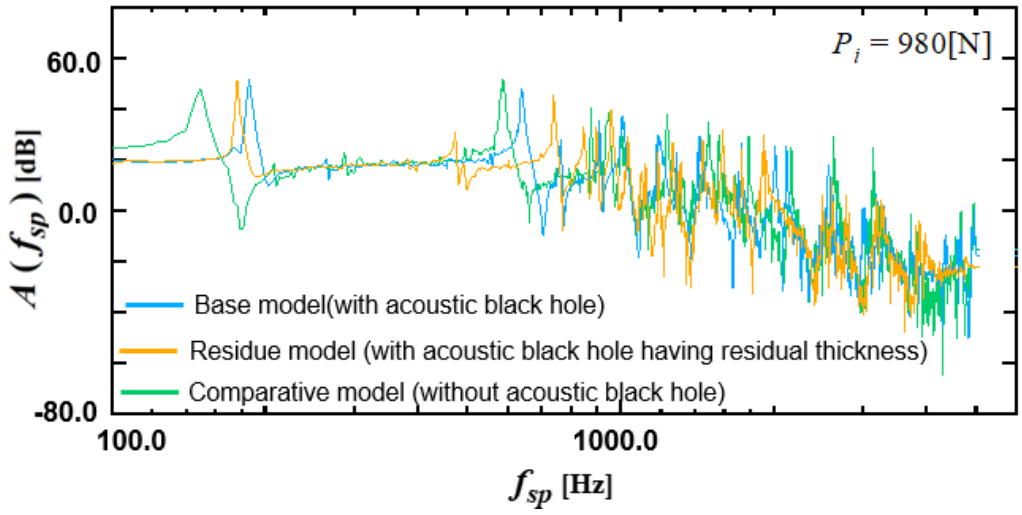

Fig. 8. Fourier spectrum of impact responses under large input (980 [N]).

To clarify quantitively effects of the residual thickness in actual structures with the acoustic black hole, it is necessary to add parameter studies under many conditions. Further, we will carry out measurement corresponding to the results in this paper as our future work.

It is important to perform sensitivity analysis for residual thickness and nonlinear spring stiffness to clarify the effects of these parameters on the nonlinear responses and optimize our proposed structure. In this paper, we showed basic and typical phenomena for our proposed structure with acoustic black hole. In our future work, we will try the sensitivity analysis of these parameters.

5. Conclusion

We proposed a lightweight, highly vibration damping structure using a new acoustic black hole that solves problems of weakness in strength. Rather than plate thickness, the acoustic black hole function was used for the height of ribs in T-shaped structures. Eigenvalue analysis and impact response analysis were performed when an acoustic black hole and an acoustic black hole with residual thickness were added to T-shaped structures supported by a nonlinear spring. And the results were compared. There exists viscoelastic damping layer on the region of acoustic black hole, but no damping layer was on the flange of the T-shaped structure.

By adding an acoustic black hole to the T-section structure, modal loss factors increased significantly. Furthermore, by adding a residual thickness to the acoustic black hole, a higher modal loss factors were obtained.

It was shown that by increasing the excitation force, high frequency components and fractional harmonic components due to nonlinear elements appear. And, by nonlinear impact response analysis, it was confirmed that peaks in the high frequency range was reduced by adding the acoustic black hole.

References

[1] M.A. Mironov, “Propagation of a flexural wave in a plate whose thickness decreases smoothly to zero in a finite interval”, ***Soviet Physics-Acoustics*** Vol.34, pp.318–319, 1988.

[2] V.V. Krylov, “Laminated plates of variable thickness as effective absorbers for flexural vibrations”, ***Proceedings of the 17th International Congress on Acoustics***, Rome, Vol. 1, 2001, 270.

[3] V.V. Krylov, F.J.B.S. Tilman, "Acoustic 'black holes' for flexural waves as effective vibration dampers", ***Journal of Sound and Vibration***, Vol.274 (3–5), pp.605–619,2004.

[4] V.V. Krylov, "New type of vibration dampers utilizing the effect of acoustic black holes.", ***Acta Acustica united with Acustica***, 90 (5) (2004) 830-837.

[5] V.V. Krylov, V. Kralovic, D.J. O'Boy, "Damping of flexural vibrations in rectangular plates using the acoustic black hole effect", ***Journal of Sound and Vibration***, Vol.329, pp.4672-4688, 2010.

[6] H. Oberst, ***Akustische Beihefte*** , Helt 4, pp.181-194,1952.

[7] L. Tang, L. Cheng, H. Ji, J. Qiu, "Enhanced Acoustic Black Hole Effect Using a Modified Thickness Profile", ***Proceedings of inter noise conference 2016***, Hamburg, 2361-2369, (2016).

[8] T. Yamaguchi, Y. Fujii, K. Nagai and S. Maruyama, "FEM for vibrated structures with non-linear concentrated spring having hysteresis", ***Mechanical Systems and Signal Processing***, Vol.20, pp. 1905-1922, 2006.

[9] T. Yamaguchi, T. Saito, K. Nagai, S. Maruyama, Y. Kurosawa and S. Matsumura, "Analysis of damped vibration for a viscoelastic block supported by a nonlinear concentrated spring using FEM", ***Journal of Environment and Engineering***, Vol. 2 (3), pp. 578-589, 2007.

[10] T. Yamaguchi, H. Hozumi, Y. Hirano, K. Tobita, and Y. Kurosawa, "Nonlinear transient response analysis for double walls with a porous material supported by nonlinear springs using FEM and MSKE method", ***Mechanical Systems and Signal Processing***, Vol.42, pp.115-128, 2014.

[11] T. Yamaguchi, C. Kamio, S. Maruyama, T. Tanaka and R. Fujinuma, "Nonlinear response analysis for T-shaped structures having new acoustic black hole with residual thickness supported by nonlinear springs", ***Journal of Mechanical and Electrical Intelligent System***, Vol. 8(1), pp. 12-23, 2025.

[12] L., Tang and L. Cheng, "Impaired sound radiation in plates with periodic tunneled Acoustic Black Holes", ***Mechanical Systems and Signal Processing***, Vol.135, pp.1-13, 2020.

[13] J. Deng, O. Guasch, L. Maxit and L. Zheng, "Transmission loss of plates with multiple embedded acoustic black holes using statistical modal energy distribution analysis", ***Mechanical Systems and Signal Processing***, Vol.150, pp.1-18, 2021.

[14] J. Deng, X. Chen, Y. Yang, Z. Qin and W. Guo, "Periodic additive acoustic black holes to absorb vibrations from plates", ***International Journal of Mechanical Sciences***, Vol.267, pp.1-14, 2024.

[15] C. D. Johnson and D. A. Kienholz, "Finite element prediction of damping structures with constrained viscoelastic layers", ***AIAA Journal***, Vol.20(9), pp.1284-1290, 1982.

[16] B. A. Ma, and J. F. He, "A finite element analysis of viscoelastically damped sandwich plates", ***Journal of Sound and Vibration***, Vol.152(1), pp.107-123, 1992.